www.vbripress.com, www.amlett.org, DOI: 10.5185/amlett.2012.12481 Published online by the VBRI press in 2013

Effect of morphology on thermal stability of core-shell polyaniline/TiO_2 nanocomposites

Ameena Parveen[1], Aashis S. Roy[2*]

[1]*Department of Materials Science, Gulbarga University, Gulbarga 585106, India*
[2]*Department of Physics, Govt First Grade College, Gurmethkal, Yadgir 584 214, India*

[*]Corresponding author. Tel: (+91) 973915480; Fax: (+91) 8472263202; E-mail: aashis_roy@rediffmail.com

Received: 06 December 2012, Revised: 15 February 2013 and Accepted: 23 February 2013

ABSTRACT

Polyaniline/TiO_2 nanocomposites have been prepared by sol-gel technique using citric acid and saturated solution of α-dextrose as a surfactant in presence of hydroxyl group at an anomeric position in sugar chain. The FTIR spectrum indicates the benzenoid, quinoid and MO peaks confirm the formation of PANI/TiO_2 nanocomposites. The XRD studies show the monoclinic structure and the TEM study of nano TiO_2 reveals that the average particles size is 9 ±2 nm whereas the composite size is 13 ± 2 nm and further it is observed that the TiO_2 nanoparticles are intercalated to form a core shell of PANI. The formation of core shell is significant up to 30wt% observed from the SEM. The TGA-DSC curves show the thermal stability of polyaniline and its nanocomposites at 660 ˚C of temperature. Copyright © 2013 VBRI press.

Keywords: Polyaniline; nano-titanium dioxide; α-dextrose; citric acid; TGA; DSC.

Ameena Parveen completed M.Sc and Ph.D in physics, Gulbarga University, Gulbarga, India. Presently working as Assistant Professor in Physics, Govt First Grade College Guirmitkal, Yadgir, India. Research interest is Synthesis of Nanomaterials, Porous Metal Oxide, Conducting Polymer Nanocomposites, Chemical Sensors, Microwave Studies, Modulous Spectroscopy and Fabrication of Organic Photovoltaic cells.

Aashis. S. Roy got his M.Sc and Ph.D degree in Materials Science from Gulbarga University, Gulbarga, Karnataka, India. He is working as Research Associate in Department of Materials Engineering, Indian Institute of Science, Bangalore, India. Research interest is Humidity Gas Sensors Applications, Development of Conducting Polymer Ceramic Nanocomposites and to Fabricate the Gas Sensors and Organic Photovoltaic Devices.

Introduction

The conducting polyaniline (PANI) has been recognized to be the most important and has exhibited great potential for commercial applications due to its unique electrical, optical and photoelectrical properties, as well as its ease of preparation and excellent environment stability **[1-3]**. Nanocrystalline TiO_2 has also been frequently used for preparing various nanocomposites with conducting polymers owing to its excellent physical and chemical properties, and promising applications in advanced coating, sensor, solar cell, photo catalyst, and so on **[4]**. Therefore, PANI/ TiO_2 nanocomposites have been most intensively studied among various nanocomposites, because it could combine the merits of PANI and nanocrystalline TiO_2 particles within a single material and are expected to find applications in electrochromic devices, nonlinear optical system, sensors and photoelectrochemical devices **[5-7]**. Most of the properties of these materials are based on the synergism between the properties of the components are a direct result from their chemical and structural composition and so they can be tailored. For instance, coatings based on organic–inorganic hybrid materials are capable to combine the flexibility and easy processing of polymers with the interesting properties of the inorganic part: hardness, thermal stability, electrical and electrochemical distinguished properties. The thermal stability of PANI base form is much higher than that of the others due to its conjugated stiff backbone and absence of counter ions. For its salt forms, their thermal stability increases with the

increase of dopant size. Nevertheless, PANI–HCl and PANI–XSA have relatively less weight loss at high temperature because of the relatively low molecular weight of their dopants **[8-9]**.

The structural study also carried by employing differential scanning calorimetry (DSC) of conductive composite films of EVA copolymer and PANI-DBSA complex, cast from water-xylene medium, PANI-DBSA being prepared in situ by oxidative polymerization of aniline in presence of DBSA. During processing and storage, such composites can be exposed to elevated temperature and changes in their structure can take place (chain defects, crosslinking, etc.). Thus, we consider that the thermal analysis is important for elucidating the interactions among the three constituents in the systems studied (PANI, DBSA and EVA copolymer) which are responsible for the structural changes, phase transitions and electrical conductivity of the composites **[10, 11]**.

The combination of nanocrystalline TiO_2, and polyaniline-TiO_2 nanocomposites is attractive because of the combination of polyaniline and metal oxide exhibits excellent electrical, mechanical and optical properties such as surface hardness, modulus, strength, transparency, high refractive index and acids and their derivatives are highly promising coupling molecules that allow the anchoring of organic groups to inorganic solids **[12-15]**. In this paper, author reports the synthesis of core-shell structured polyaniline/TiO_2 nanocomposites. The prepared samples were characterized by FTIR, XRD, SEM and TEM. Effect of core shall morphology on thermal properties of prepared composites is elucidated.

Experimental

Materials

All Chemicals used were analytical grade (AR). The monomer aniline was doubly distilled prior to use. Ammonium persulphate ($(NH_4)_2S_2O_8$), hydrated titanium nitrate (TiO_2 $(NO_3)_2.6H_2O$), hydrochloric acid (HCl) were procured from Sigma Aldrich and were used as received.

Synthesis of polyaniline

Aniline (0.1mol) was dissolved in 1M HCl to form aniline hydrochloride solution. To this reaction mixture, 0.1M of ammonium persulphate [$(NH4)_2S_2O_8$] which acts as an oxidant was added slowly with continuous stirring at 0–5^{0}C. After complete addition of the oxidizing agent, the reaction mixture was allowed to keep for 24 h without stirring. The greenish black precipitate of the polyaniline was recovered by vacuum filtration and washed with acetone and 0.1N HCl in order to remove the oligomers and chlorine ions respectively. The precipitate was dried in an oven for 24 h at 50 ^{0}C to achieve constant weight.

Preparation titanium dioxide

Two step sol-gel preparation methods are used to synthesize nano TiO_2 which has been described as follows. In the first step, 160 ml of 0.1N titanium nitrate hydrated [TiO_2 $(NO_3)_2.6H_2O$] and 480 ml of 0.1N citric acid are mixed thoroughly by stirring at room temperature. To this mixture, ammonia is added drop-wise with constant stirring using magnetic stirrer for 5-6 h at room temperature. The purpose of adding ammonia is to maintain the pH at 4. Finally, a gel is formed. In the second step, the saturated solution of alpha dextrose is added to above gel and stirred for 2h at 120^{0}C which turns to a spongy type solid residue. This spongy gel is ignited at a temperature of about 300^{0}C for 1h in air ambient. Finally, fine graded TiO_2 nanoparticles are formed.

Preparation of composite

Aniline hydrochloride / [TiO_2 $(NO_3)_2$ $6H_2O$] / citric acid are taken in the molar ratio of 1:2: 3 and are stirred thoroughly for 1h at 25^{0}C. To this mixture, ammonium persulphate [$(NH_4)_2S_2O_8$] as oxidant and saturated solution of α–dextrose is added with constant stirring at 70 ^{0}C for 5-6 h which acts as surfactant because of a free hydroxyl group present at the anomeric position exist as an equilibrium mixture between acyclic and cyclic forms. It finally gives a green gel precipitate **[16 -17]**. The gel is further refluxed with 0.1N HCl to enhance the protonation processes and then vigorously washed with distilled water and acetone to remove the excess α-dextrose, citric acid and oligomers from the composite. Further, the composite is dried at 80^{0}C for 5-6 h to achieve constant weight. The various weight percentages of 10, 20, 30, 40 and 50 wt % of Polyaniline/TiO_2 nanocomposites have been prepared by same method.

The pellets of 10 mm diameter are prepared with thickness varying up to 2 mm by applying pressure of 1Tons in a UTM – 40 (40 Ton Universal testing machine). For temperature dependent conductivity, the pellets are coated with silver paste on either side of the surfaces to obtain better contacts.

Characterization

Infrared spectroscopy

The IR spectra of all the samples are recorded on Perkin Elmer (model 783) IR spectrometer in KBr medium at room temperature. For recording IR spectra, powders are mixed with KBr in the ratio 1:25 by weight to ensure uniform dispersion. The mixed powders are pressed in a cylindrical dye to obtain clean discs of approximately 1 mm thickness.

X-ray diffraction

X-ray diffraction Phase identification was carried out by a Shintag X1 diffractometer with Cu K_α (1.54 A^0) radiation in θ – θ configuration at ambient emperature. The patterns were recorded in the 2-70^0 range at 0.05^0 step size using 3-s acquisition time per step. The mean particle size (PS) was calculated using the Debye–Scherrer equation given below. where K is a constant equal to 0.9 λ is the wavelength of the Cu K_α radiation, β is the half-peak width of the diffraction peak in radiant and θ is the Braggs angle of (311) plane.

$$PS = 0.9\,\lambda / \beta\,\mathrm{Cos}\,\theta \qquad (1)$$

where β is full width half maxima, θ is angle of reflection.

Scanning electron microscopy and transmission electron microscopy

The powder morphology of polyaniline and its composites sintered in the form of pellets (to measure grain size) are investigated using Phillips XL30 ESEM scanning electronic microscope (SEM). The samples in the form of pellets are mounted on aluminum plat form and conducting gold is sputtered on the sample to avoid charging at the sample surfaces and hence selected areas were photographed. The particle morphology of polyaniline and its composites sintered in the form of pellets are investigated employing JEOL 2000 FX–II TEM was used at an accelerating voltage of 200 kV.

Thermogravimetric-differential scanning calorimeter (TG-DSC)

Thermal studies (TG/ DSC measurements) were performed on Linseis STA PT-1600 (Germany) Thermal analyzer.10mg of completely dried sample is taken in a clean alumina crucible and heated up to 50°C - 700 °C in the nitrogen atmosphere at the rate of 10° C/min.

Results and discussion

Infrared Spectroscopy

Fig. 1(a-c) shows FTIR spectra of pure polyaniline and polyaniline/TiO_2 nanocomposites. The vibrational bands are found to be at 503 cm^{-1}, 808 cm^{-1}, 1133 cm^{-1}, 1294 cm^{-1}, 1491 cm^{-1} and 1581 cm^{-1}. The bands at 503 cm^{-1} and 808 cm^{-1} are due to C–H out-of-plane bending vibration and para disubstituted aromatic rings, respectively. A band appearing near 1294 cm^{-1} represents the C–N stretching vibration. The C–H in the plane bending vibration occurs at 1133 cm^{-1}.

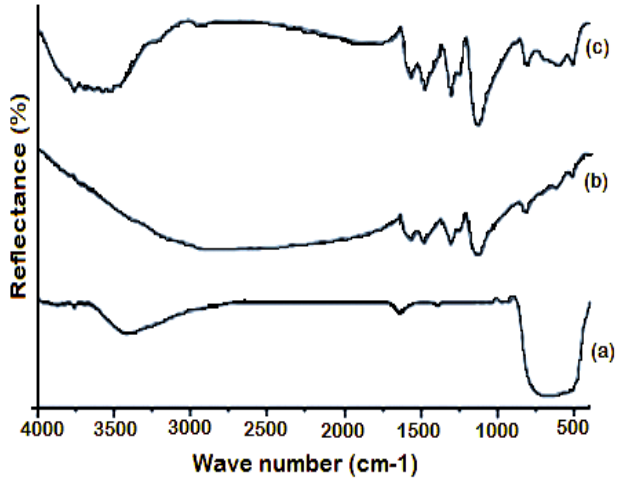

Fig. 1 (a-c) Shows the FTIR spectra of polyaniline, pure nano TiO_2 and polyaniline / TiO_2 nanocomposites.

The presence of two bands in the range of 1450–1600 $cm^{-1}$is assigned to the non-symmetric C_6 ring stretching modes. The higher frequency vibration at 1581 cm^{-1} has a major contribution from the quinoid rings, while the lower frequency mode at 1491 cm^{-1} depicts the presence of benzenoid rings. The broad band observed at 3280–3500 $cm^{-1}$is due to the N–H stretching of aromatic amines and at 2500–3000 cm^{-1} is due to aromatic C–H stretching vibrations. Thus an FTIR spectra peak confirms the formation of composites and also suggests a Vander walls kind of interaction between the polymeric chain and TiO_2 nanoparticles.

X-ray diffraction

Fig. 2 (a-c) shows the XRD patterns of polyaniline / TiO_2 nanocomposite respectively. **Fig. 2 (a)** reveals that the polyaniline is amorphous in nature. An intensity peak is found to be around 26° for polyaniline which may be assigned due to the scattering of polyaniline chains at interplanar spacing. When $(NH_4)_2S_2O_8$ is added to the reaction system, it is observed that polymerization proceeds initially on the surface of TiO_2 nanoparticles due to the restrictive effect of the surface and there after polyaniline encapsulates the crystalline behavior of polyaniline / TiO_2 nanocomposite which are hampered. Therefore, the degree of crystallinity of polyaniline decreases and the diffraction peaks emerged with TiO_2 peaks and hence cannot be distinguished. Comparing the curves of pure TiO_2 and polyaniline/TiO_2 nanocomposite it is seen that polyaniline deposited on the surface of TiO_2 nanoparticles has no effect on crystallization performance .It is seen from **Fig. 2 (b- c)** that the monoclinic peaks of TiO_2 indicates the crystalline nature of the TiO_2 and PANI/TiO_2 nanocomposite. By comparing the XRD patterns of PANI/TiO_2 nanocomposite with that of TiO_2, the prominent peaks corresponding to $2\theta = 25.61^0$, 38.12^0, 47.53^0 and 54.03^0 are due to (110), (101), (111) and (211) planes which indicates the presence of TiO_2 in PANI [JCPDS file no. 21 -1276]. By comparing the XRD patterns of pure polyaniline with its composite, it is observed that TiO_2 has retained its structure even though it is dispersed in PANI after polymerization reaction.

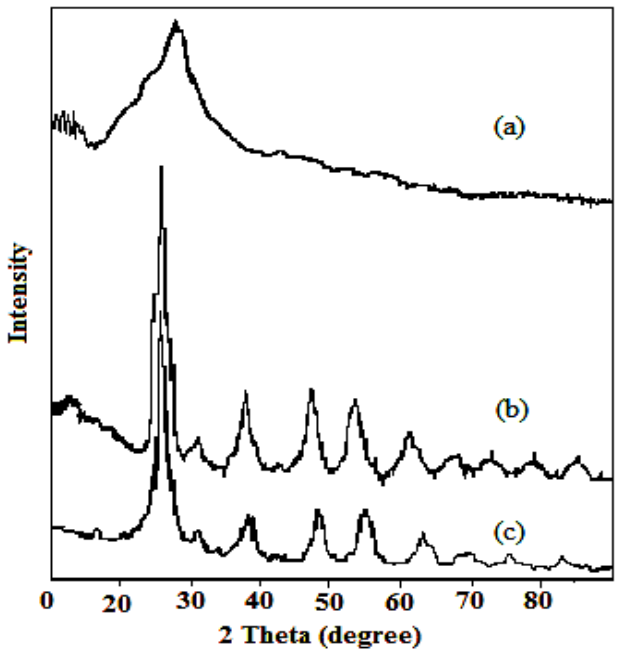

Fig. 2 (a-c) shows those XRD spectra of polyaniline, pure TiO_2 and PANI/TiO_2 nanocomposites.

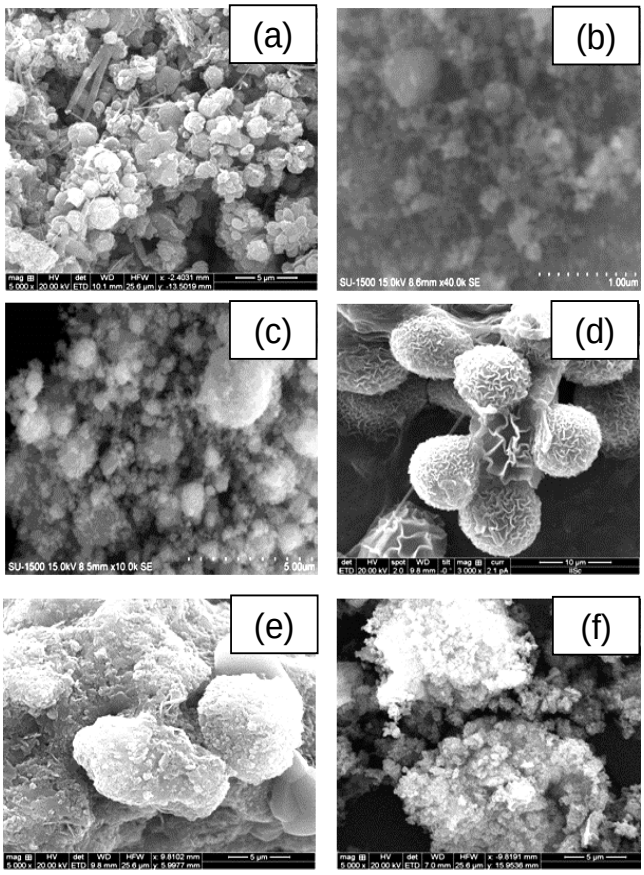

Fig. 3 (a-f) Shows the SEM image of polyaniline and PANI/TiO_2 nanocomposites at different weight percentage (10, 20, 30, 40 and 50 wt %).

Scanning electron microscopy

Fig. 3 (a) shows the SEM image of pure polyaniline at room temperature. Through careful observations, it is found that the particles are highly agglomerated and well interconnected with each other. The granular shape particles are tied with the polyaniline fibers and have an average grain size of 0.65μm. **Fig. 3 (b)** shows the SEM image of 10 wt % of gelatinous polyaniline/TiO_2 nanocomposites at the temperature of 40^0C after 4h. The particles are agglomerated into an irregular shape and have initiated the formation of a granular structure. This may be due the presence of small percentage of TiO_2 nanoparticles in polyaniline matrix. The average grain size is ranging from 0.8 μm to 1 μm. **Fig. 3(c)** shows the SEM image of 20 wt % of gelatinous polyaniline/TiO_2 nanocomposites at the temperature of 40^0C after 4h. The particles are highly clustered, homogeneous, regular and spherical in shape. Here the granular morphology itself shows the formation of PANI core-shell over the TiO_2 nanoparticles. This indicates that there was a formation of two layers over the PANI/TiO_2 nanocomposite of citric acid and α-dextrose which causes the strain in the polymer chain to form the circular structure. The average grain size is in the range of 0.6 μm to 1.5 μm. **Fig. 3(d)** shows the SEM image of 30 wt % of gelatinous polyaniline/TiO_2 nanocomposite at the temperature of 40^0C after 4h. The particles are clustered homogeneous and circular in shape and have almost similar in size. The average grain size is of about 2 μm. This clearly indicates that there is a continuous increase in the volume of the core shell with increase in percentage of nanocrystalline TiO_2 in polyaniline matrix.

Fig. 3(e) shows the SEM image of 40 wt % of gelatinous polyaniline/TiO_2 nanocomposite at the temperature of 40^0C after 4h. The particles are highly agglomerated in a semicircular fashion. The outer surface of the shell looks rough when you compared with 10, 20 and 30 wt. % of its composites. This is due to crack at outer surface of the shell which attributes to the formation of core shell more significant below 30 weight percentage of nanocrystalline titanium dioxide particle in polyaniline. Hence the average granular size decreases to 1.6 μm. **Fig. 3(f)** shows the SEM image of 50 wt % of gelatinous polyaniline/TiO_2 nanocomposite at the temperature of 40^0C after 4h. The particles are found to be loosely held with each other which cause more porosity in the composites. It is seen that the shells are completely ruptured due to predominant wt. % of nanocrystalline TiO_2 particles over the polymer matrix. This clearly indicates that the increase in nano TiO_2 nanopartciles decreases the strain in the polymer chain due to surfactant and also decreases the binding force between the particles and matrix. Therefore, the average granular size decreases up to 1.3 μm. **Fig. 3(b)** and **Fig. 3(f)** shows that formation of core-shell is more significant, if TiO_2 nanoparticles is less than 30 wt.% in polyaniline matrix than this may give a high thermal stability and good other properties. Therefore, these materials can be used in electronic device.

Transmission electron microscopy

Fig. 4(a-b) shows TEM images of TiO_2 and polyaniline/TiO_2 nanocomposites. The TEM image of polyaniline/TiO_2 nanocomposite shows the granular structures. An obtained average size of this was found to be of about 7nm and 13nm, respectively. The surface to volume ratio of TiO_2 nanoparticles decreases the size of composites from bulk to nano because the particle size decreases with an increase in the concentration of the composite. Thus polyaniline provides strength and stiffness to polyaniline/TiO_2 nanocomposite, whereas polyaniline matrix acts as a binder that distributes external load to the fibers. In addition to increasing the rigidity of the polymer matrix, the particles are added to modify rheological property. The conformational energy map of polyaniline matrix macromolecules displays a very rigid and extended structure. This may be attributed to the formation of intra residue hydrogen bonds between the molecules resulting in a randomly shaped structure.

Thermogravimetry-differential scanning calorimetric analysis (TG-DSC analysis)

The TGA-DSC curves of pure polyaniline and polyaniline/TiO_2 nanocomposites with various weight percentages is shown **Fig. 5 (a, b)**. From **Fig. 5(a)** it is found that an offset decomposition temperatures of composites were higher than that of pure PANI and shifted towards the higher temperature range as the content of nanostructured TiO_2 increased whereas the onset value

decreases because the small particles changes the rate of reaction and hence the shape of the TGA curves also altered.

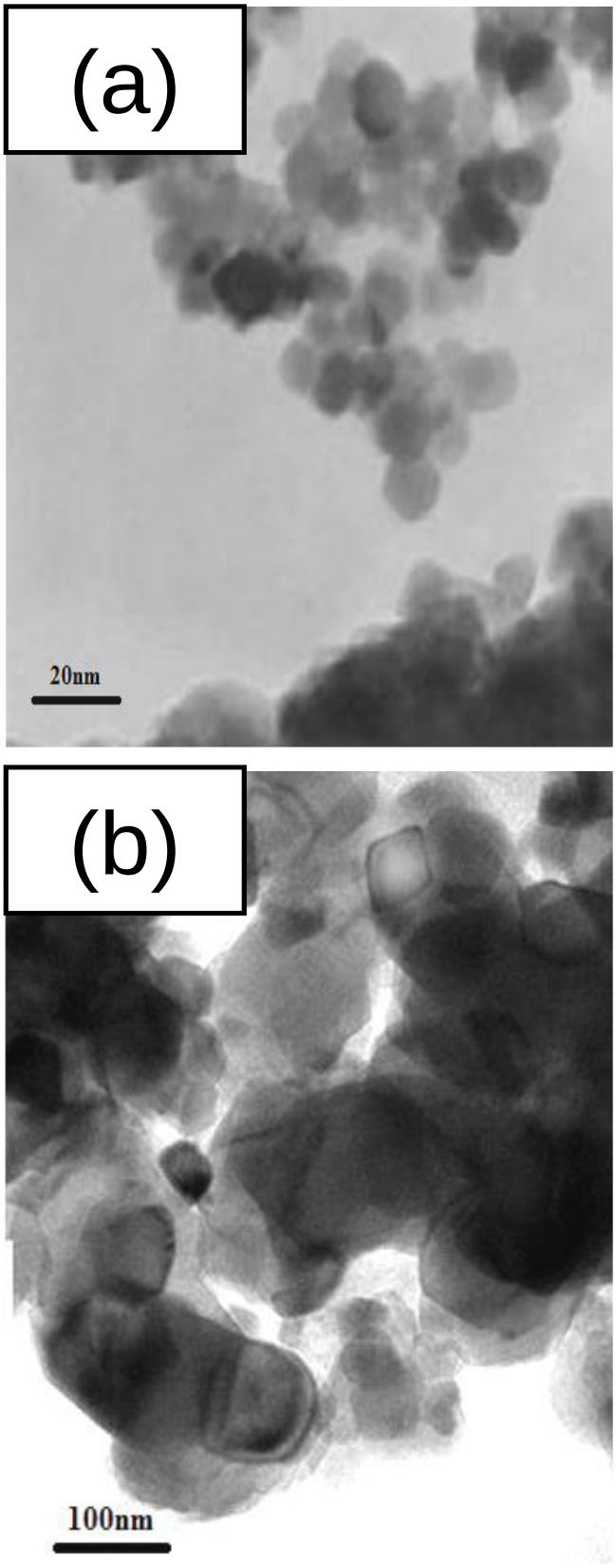

Fig. 4. shows the TEM image of (a) pure nanostructured titanium dioxide and (b) 30 wt% of polyaniline/TiO_2 nanocomposite.

The decomposition starts much earlier and comparatively low temperature of PANI with the samples having nanostructure titanium dioxide. This behavior confirmed the increased thermal stability of composites as the content of nanostructured TiO_2 is increased and that could be attributed to the retardation effect of nanostructuredTiO_2 as barriers for the degradation of PANI **[18-20]**. From the graph it is found that the onset temperature is 238.9 °C and at the offset point found is at 344.7 °C. The result agrees with the moisture evaporation which are trapped inside the polymer or bound to the polymer backbone as evidenced by the first degradation stage of TGA curve **[21]**.

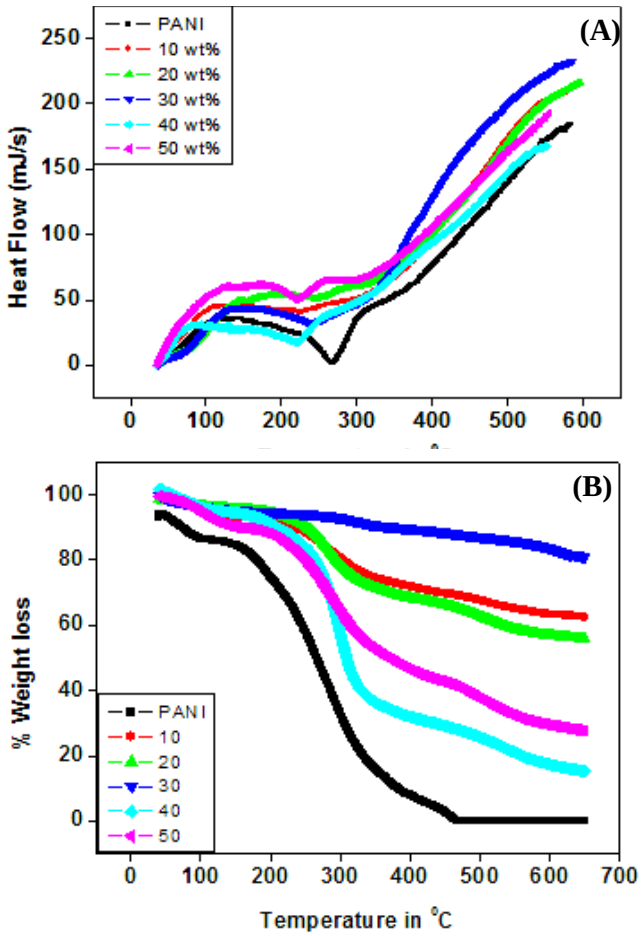

Fig. 5. (a) TGA curve of pure polyaniline and polyaniline/TiO_2 nanocomposites at different weight percentage (10, 20, 30, 40 and 50 wt %) and (b) DSC curve of pure polyaniline and polyaniline/n-TiO_2 composites at different weight percentage (10, 20, 30, 40 and 50 wt %).

It can be observed from DSC curved **Fig. 5(b)** that the thermal decomposition of polyaniline and polyaniline/TiO_2 nanocomposites curve weight percentages shows a three-stage decomposition pattern. For pure polyaniline it shows a large weight loss occurring below 650 °C and can be describe to the elimination of water, acetone and HCl. For pure polyaniline three mass losses could be detected in the temperature range of 50−650 °C. The first weight loss observed at 80 to 140 °C was essentially due to deabsorption of water absorbed on the doped polymer. The loss of 140 to 200 °C can be primarily related to the

expulsion of the doped HCl from PANI. The main loss at 200 to 450 °C can be described to thermal degradation of skeletal polyaniline chain structure. This curve also indicates that there is a sharp weight loss near 200 °C and continues until 650 °C at which PANI almost completely decomposed. The total mass change of PANI at the temperature range from 50 to 660 °C is about 86.97%. The DSC curve peaks indicates the endothermic process where energy is required to break the bonds in the successive elimination of H_2O_2 CO and CO_2.

The same behaviour is observed even for all weight percentage of polyaniline/TiO_2 nanocomposites. But 30 wt% of polyaniline/n-TiO_2 composites shows a less weight loss occurring above 650^0C and can be use for the elimination of organic moieties, water and HCl in the temperature range of 50−650 °C.

In DSC curve generally the glass transition temperature (Tg) of PANI powders is not evident in the thermographs **[22]**. The exothermic transition observed at 179.3 - 266.1 °C is believed not to be Tg. Instead it would be attributed to a series of chemical reactions. Basically bond scissioning followed by a bond formation are involved when the powders are heated. The bond scissioning is endothermic, which is compensated by the generated heat by bond formation and shows an exothermic peak at around 150 - 300 °C. The decreased peak temperatures from 273 °C (pure PANI) to 179.7, 222.5, 238.4, 245.2 and 264.2 °C for the PNCs filled with a particle loading of 30, 50, 40, 20 and 10 wt%, respectively, further demonstrate the ordered polymer structure as well as good interfacial interactions between the metal oxide and the polymer matrix.

Conclusion

The core shell of polyaniline/TiO_2 nanocomposites have been prepared by sol-gel technique using citric acid and α-dextrose as a surfactant. The higher frequency vibration at 1581 cm^{-1} has a major contribution from the quinoid rings, while the lower frequency mode at 1491 cm^{-1}, 3419 cm^{-1} and 634 cm^{-1} depicts the presence of benzenoid ring units and corresponds to Ti–O–Ti and O–H stretching frequencies. Hence the FTIR results confirm the formation of PANI/TiO_2 nanocomposite. The XRD studies show the monoclinic structure and the TEM study of TiO_2 reveals that the size is of the order of 9 nm where as the nanocomposite size it is of the order of 13nm and further it is observed that the TiO_2 nanoparticles are intercalated to form a core shell of PANI. The formation of core-shell is more significant, if TiO_2 nanoparticles less than 30 wt % in polyaniline matrix is revels from the SEM image. The TG-DSC curve shows the offset decomposition temperatures of nanocomposites were higher than that of pure PANI and shifted toward the higher temperature range as the content of nanostructured TiO_2 increased whereas the onset value decreases because the small particles change the rate of reaction and hence the shape of the TG curves also altered. This behavior confirmed the increased thermal stability of polyaniline/TiO_2 nanocomposites compared with pristine polyaniline.

Reference

1. Huang, J, Virji S, Weiller BH. Kaner RB. J Am Chem Soc; **2003**, *125*, 314-5. **DOI:** 10.1021/ja028371y.
2. A. Tiwari, S. K. Shukla, *e-XPRESS Poly. Let*, **2009**, 3, 553–559 **DOI:** 10.3144/expresspolymlett.2009.69
3. Huang J X, Kaner R B, J Am Chem Soc; **2004,** *126*, 851-5. **DOI:** 10.1021/ja0371754
4. Deore BA, Yu I, Freund MS. J Am Chem Soc; **2004**, 126, 52-3. **DOI:** PMID 14709055
5. A. Tiwari, J. Macrom. Sci. A, **2007**, 44, 735–745 **DOI:** 10.1080/10601320701353116
6. A. Roy, A. Parveen, R. Deshpande, R. Bhat, A. R. Koppalkar, J. Nanopart. Res, **2013**, 15, 1337. **DOI:** 10.1007/s11051-012-1337-z
7. A. S. Roy, K. R. Anilkumar, M. V. N. Ambika Prasad, J. Appl. Poly. Sci, **2011**, 123, 1928–1934 **DOI:** 10.1002/app.34696
8. Khanna P K, Kulkarni MV, Singh N, Lonkar SP, Subbarao VS, Viswanath AK. Mater. Chem. Phys; **2006,** *95*, 24-8. **DOI:** 10.1021/cm203132m
9. Y. B. Wankhede, S. B. Kondawar, S. R. Thakare, P. S. More, Adv. Mat. Lett. **2013**, 4, 89- 93 **DOI:** 10.5185/amlett.2013.icnano.108
10. Long YZ, Chen ZJ, Duvail JL, Zhang ZM, Wan MX. Physica B, **2005**, *370*, 121- 130. **DOI:** 10.1016/j.physb.2005.09.009
    Tiwari, A.; Sharma, Y.; Hattori, S.; Terada, D.; Sharma, A. K.; Turner, A.P.F.; Kobayashi, H. *Biopolymers*, **2013**, *99*, 334.
11. Biswas M, Sinha RS, Liu YP. Synth. Met; **1999**, *105*, 99-105. **DOI:** 10.1016/S0379-6779(99)00049-1
12. A. Tiwari, V. Sen, S. R. Dhakate, A. P. Mishra and V. Singh, Polym. Adv. Technol. 2008, 19: 909–914 **DOI:** 10.1002/pat.1058.
    Tiwari, A.; Gong, S. *Talanta*, **2009**, *77*, 1217.
    Tiwari, A.; Gong, S. *Electroanalysis*, **2008**, *20*, 1775.
    Tiwari, A.; Singh, V. *Carbohydrate Polymers*, **2008**, *74*, 427.
    Tiwari, A.; Singh, V. *Express Polymer Letters*, **2007**, *1*, 308.
    Tiwari, A.; Kumar, R.; Prabaharan, M.; Pandey, R. R.; Kumari, P.; Chaturvedi, A.; Mishra, A. K. *Polymers for Advanced Technologies*, **2010**, 21, 615.
13. B. I. Nandapure1, S. B. Kondawar, M.Y. Salunkhe, A. I. Nandapure, Adv. Mat. Lett. **2013**, 4, 134-140 **DOI:** 10.5185/amlett.2012.5348
14. Feng W, Sun EH, Fujii A, Wu HC, Niihara K, Yoshino K. Bull. Chem. Soc. Jpn; **2000**, *73*, 2627-33. **DOI:** 10.1016 /S0008-6223(03)00078-2
15. Zhang L J, Wan M X, Wei Y, Synth. Met; **2005**, *151*, 1-5. **DOI:** 10.1016/j.synthmet.2004.12.021
16. Park S J, Park S Y, Cho M S, Choi H J, Jhon MS. Synth. Met. **2005**, *152*, 33-40. **DOI:** 10.1016/J.SYNTHMET.2005.07.085
17. Tsocheva1 D, Tsanov T, Terlemezyan L. Journal of Thermal Analysis And Calorimetry; **2001**, *66*, 415- 22.
    Shukla, S. K.; Vamakshi, Minakshi, Bharadavaja, A.; Shekhar, A.; Tiwari, A. *Advanced Materials Letters*, **2012**, *3*, 421.
18. Nagaveni K, Hegde MS, Ravishankar N, Subbanna GN, Madras G. Langmuir, **2004**, *20*, 2900-7. **DOI:** 10.1021/la702504v.
19. Deng J G, He CL, Peng YX, Wang JH, Long XP, Li P, Synth. Met; **2003**, *139*, 295. **DOI:** 10.1016/S0379-6779(03)00166-8
20. Li XW, Wang GC, Li XX, Lu DM. Appl. Surf .Sci; **2004**, *229*, 395-401 **DOI:** 10.1016/j.apsusc.2004.02.022
21. Narayan H, Alemu H, Iwuoha E. Phys. Status Solidi A, **2006**, *203*, 3665-72. **DOI:** 10.1002/pssa.200690022
    Singh, R.P.; Tiwari, A.; Pandey, A. C. *J Inorg Organomet Polym*, **2011**, *21*, 788.
22. Yanni Qi, Jian Zhang, Shujun Qiu, Lixian Sun, Fen Xu, Min Zhu, Liuzhang Ouyang, Dalin Sun. J Therm. Anal. Calorim. **2009**, *98*, 533–537. **DOI:** 10.1007/s10973-009-0298-7
    Shukla, S. K.; Bharadvaj, A.; Tiwari, A.; Parashar, G. K.; Dubey, G. C. *Adv Mat Lett*, *1*, **2010**, 129.
    Shukla, S.K.; Tiwari, A. *Advanced Materials Research*, **2011**, *306-307*, 82.